Available online at www.sciencedirect.com
SCIENCE DIRECT®
Developmental Biology 267 (2004) 190–202
DEVELOPMENTAL BIOLOGY
www.elsevier.com/locate/ydbio

# Cre-mediated excision of *Fgf8* in the *Tbx1* expression domain reveals a critical role for *Fgf8* in cardiovascular development in the mouse

Christopher B. Brown,[a] Jennifer M. Wenning,[a] Min Min Lu,[a] Douglas J. Epstein,[b] Erik N. Meyers,[c] and Jonathan A. Epstein[a,*]

[a] *Cardiovascular Division, Department of Medicine, University of Pennsylvania, Philadelphia, PA 19104, USA*
[b] *Department of Genetics, University of Pennsylvania, Philadelphia, PA 19104, USA*
[c] *Department of Pediatrics, Neonatal–Perinatal Research Institute, Duke University Medical Center, Durham, NC 27710, USA*

Received for publication 22 August 2003, revised 13 October 2003, accepted 15 October 2003

**Abstract**

*Tbx1* has been implicated as a candidate gene responsible for defective pharyngeal arch remodeling in DiGeorge/Velocardiofacial syndrome. *Tbx1*$^{+/-}$ mice mimic aspects of the DiGeorge phenotype with variable penetrance, and null mice display severe pharyngeal hypoplasia. Here, we identify enhancer elements in the *Tbx1* gene that are conserved through evolution and mediate tissue-specific expression. We describe the generation of transgenic mice that utilize these enhancer elements to direct Cre recombinase expression in endogenous Tbx1 expression domains. We use these *Tbx1-Cre* mice to fate map *Tbx1*-expressing precursors and identify broad regions of mesoderm, including early cardiac mesoderm, which are derived from *Tbx1*-expressing cells. We test the hypothesis that fibroblast growth factor 8 (*Fgf8*) functions downstream of *Tbx1* by performing tissue-specific inactivation of *Fgf8* using *Tbx1*-Cre mice. Resulting newborn mice display DiGeorge-like congenital cardiovascular defects that involve the outflow tract of the heart. Vascular smooth muscle differentiation in the great vessels is disrupted. This data is consistent with a model in which Tbx1 induces *Fgf8* expression in the pharyngeal endoderm, which is subsequently required for normal cardiovascular morphogenesis and smooth muscle differentiation in the aorta and pulmonary artery.


*Keywords:* *Fgf8*; *Tbx1*-Cre mice; DiGeorge syndrome

## Introduction

The pharyngeal arches are transient embryonic structures that give rise to the ventral regions of the head and neck. The pharyngeal arches arise as ventrolateral outpouches. Each arch consists of a mesodermal core covered with an outer layer of ectoderm and an inner layer of endoderm. The arches are invaded by neural crest cells that remodel the primitive structure and form mature tissues including bone, nerve, connective tissue, and smooth muscle. The parathyroids and thymus are derived from the endoderm of the pharyngeal pouches with contributions from neural crest (Graham, 2001; Graham and Smith, 2001). Contained within the arches are a series of initially bilaterally symmetric arteries that are remodeled to form the mature asymmetric aortic arch arteries. The formation and remodeling of the pharyngeal arches and associated arch arteries are a result of complex molecular interactions between the mesodermally derived arch core mesenchyme, ectoderm, endoderm, and neural crest cells (Hiruma et al., 2002). Observations of pharyngeal patterning abnormalities secondary to a specific genetic mutation might reflect defects in ectoderm, mesoderm, endoderm, or neural crest. Defects may reflect a primary defect in a given tissue layer or defective signaling between tissue types.

DiGeorge syndrome is a common human haploinsufficient disorder affecting pharyngeal arch development and patterning. DiGeorge syndrome is characterized by decreased or absent parathyroid and thymus, craniofacial abnormalities, and conotruncal and aortic arch cardiac defects (Epstein, 2001; Goldmuntz and Emanuel, 1997). The T-box transcription factor *TBX1* has recently been described as a candidate gene for DiGeorge syndrome.

* Corresponding author. Cardiovascular Division, Department of Medicine, University of Pennsylvania Health System, 954 BRB II, 421 Curie Boulevard, Philadelphia, PA 19104. Fax: +1-215-573-2094.
*E-mail address:* epsteinj@mail.med.upenn.edu (J.A. Epstein).

0012-1606/$ - see front matter © 2003 Elsevier Inc. All rights reserved.
doi:10.1016/j.ydbio.2003.10.024

Targeted inactivation of *Tbx1* in mice results in DiGeorge-like cardiovascular, thymic, and parathyroid defects in embryos heterozygous for the mutation. *Tbx1* nulls display a more complete pharyngeal arch phenotype including severe hypoplasia of the thymus and parathyroid, craniofacial and skeletal abnormalities, and cleft palate in addition to cardiovascular malformations (Jerome and Papaioannou, 2001; Lindsay et al., 2001; Merscher et al., 2001).

*Tbx1* is a member of the T-box family of transcription factors. The expression pattern of *Tbx1* is consistent with a role in pharyngeal arch and pouch remodeling (Garvey et al., 1996). As the pharyngeal arches are forming between E9 and 11 in the mouse, *Tbx1* is expressed in the head mesenchyme and mesenchyme dorsal to the pharynx as well as the mesenchymal cores of pharyngeal arches 1–3. *Tbx1* is expressed in the epithelium of the otic vesicle and in the epithelium of the endodermal pouches (Garvey et al., 1996). Endodermal expression in the pharyngeal pouches is temporally regulated such that expression is first noted in pouch 1, followed by sequential expression in more caudal pouches (Vitelli et al., 2002a). Expression is also observed in the sclerotome of the developing somite, consistent with the skeletal defects seen in *Tbx1* null mice (Jerome and Papaioannou, 2001).

*Tbx1* affects developmental processes in both cell autonomous and cell nonautonomous fashions. This bimodal activity of *Tbx1* is evident in the phenotype of DiGeorge syndrome and in targeted *Tbx1* mice. In the pharyngeal endoderm, *Tbx1* is presumed to act cell autonomously to directly regulate the development of the thymic and parathyroid precursor cells in which it is expressed (Jerome and Papaioannou, 2001; Merscher et al., 2001). The function of *Tbx1* in regulating development of other pharyngeal structures has been less clear. While *Tbx1* is broadly expressed in mesodermal tissues including the head mesenchyme and the mesenchymal cores of the pharyngeal arches, these areas are heavily invested with and remodeled by neural crest cells that give rise to the bulk of the mature structures (Graham, 2001; Graham and Smith, 2001). Results from our lab and others have shown that *Tbx1* is not expressed in the neural tube or neural crest cells (Kochilas et al., 2002; Vitelli et al., 2002a). Thus, a primary role of *Tbx1* in pharyngeal development may be to regulate expression of secreted signaling factors required for migration, differentiation, and maintenance of neural crest cells.

Recent reports have suggested that *Tbx1* expression in pharyngeal pouch endoderm regulates expression of secreted *Fgf8* (Abu-Issa et al., 2002; Frank et al., 2002; Kochilas et al., 2002; Vitelli et al., 2002b). In *Tbx1* nulls, *Fgf8* is down-regulated in *Tbx1* expression domains such as the pharyngeal endoderm, while *Fgf8* expression is unaltered in surface ectoderm that does not normally express *Tbx1*. *Fgf8* hypomorphic mice display defects in aortic arch patterning similar to those seen in *Tbx1*-deficient animals. Defective aortic arch patterning in the *Fgf8* hypomorphs may be due to inappropriate cell death or differentiation of the invading neural crest cells caused by a loss of *Fgf8* from the underlying endoderm (Abu-Issa et al., 2002 and Frank et al., 2002). It remains unclear whether *Fgf*s have direct long-range effects on cardiac neural crest cells, or if they activate secondary signaling cascades within the pharyngeal mesenchyme, which subsequently signal to the neural crest. Patterning of mesenchyme by an adjacent layer of epithelium is a common mechanism utilized in the formation of many tissues throughout embryogenesis (Johnson et al., 1994).

To better understand the role of *Tbx1* and downstream signaling pathways in aortic arch patterning, we have analyzed the *cis*-control elements regulating *Tbx1* gene expression in murine embryos and we have identified separable regions regulating gene expression. We have utilized *Tbx1* regulatory elements to generate transgenic mice expressing Cre-recombinase in the *Tbx1* expression domain. Fate-mapping studies utilizing these mice provide new insights into the extent of the contributions of cells of the *Tbx1* lineage to mature structures. We demonstrate that targeted inactivation of *Fgf8* in the *Tbx1* domains results in a spectrum of cardiovascular defects reminiscent of DiGeorge syndrome, confirming a role for *Fgf8* in cardiovascular patterning, demonstrating that FGF8 production fromTbx1 expressing cells is required for normal cardiovascular patterning.

## Materials and methods

### *Transgenic analysis*

*Tbx1* cDNA sequences were used to identify human and mouse genomic sequences in the NCBI database. Regions of sequence homology were identified by direct human–mouse sequence comparison. Fragments were amplified by PCR from SV129 mouse genomic DNA using LA-Taq DNA polymerase (TAKARA). Fragments were subcloned into a modified pBluescript vector containing a *lacZ*-coding region and SV40 poly A using a subcloning strategy in which the 5′ primer incorporated *Xho*I and *Bam*HI restriction sites while the 3′ primer incorporated a *Bgl*II site. Fragments are defined in Fig. 1. The somite enhancer was identified by serial deletion analysis and represents the 5′ most 207 bp of enhancer fragment 1, a

*Tbx1* Fragment 1 Forward:
GGCTCGAGACGGGCACCAGGCAGTCCTGTG
*Tbx1* Fragment 1 Reverse:
CGGGATCCTTCACTGCCTATGTTACCTCTTTTAATGTGGC
Fragment 1: 3547 bp

*Tbx1* Fragment 2 Forward:
CCGCTCGAGCGCGGATCCACACACTGTGGGGTGGCTTCTG
*Tbx1* Fragment 2 Reverse:
CAGCAGAACAGGGTATAGAGGCTCTGTGGG
Fragment 2: 772 bp

*Tbx1* Fragment 3 Forward:
CCGCTCGAGCGCGGATCCTGACAGTACCTGGGGTAAGGGA
*Tbx1* Fragment 3 Reverse:
CGAAGATCTCCCAGGTCACCAGGGCCCCCTGCGGTCTAGA
Fragment 3: 222 bp

*Tbx1* Proximal Forward:
CCGCTCGAGCGCGGATCCAGCGACGGTGCTGGGTGCAGCC
*Tbx1* Proximal Reverse:
GGAGATCTGGTAGCCGGCGAAGTTTCGCCC
Proximal: 3129 bp

region highly conserved between mouse and human sequences (Fig. 1A).

Enhancer-*lacZ* constructs were purified by restriction digestion and gel purification. Pronuclear injections for generation of transgenic animals were performed by the University of Pennsylvania mouse transgenic core or the Cardiology Division mouse transgenic core. Expression patterns were assayed following overnight incubation in X-gal (5′-bromo-4-chloro-3-indolyl-β-D-galactopyranoside). Protocols are available online at http://www.uphs.upenn.edu/mcrc. To establish stable lines, the 7.6-kb *Tbx1* sequence used to produce *Tbx1-lacZ* construct A (Fig. 1B) was subcloned into either *lacZ* or Cre-recombinase expression vectors.

### *Generation of Tbx1-Cre::R26R embryos*

To lineage trace *Tbx1*-Cre expressing cells, potential *Tbx1*-Cre founders were identified by PCR and mated to homozygous R26R reporter mice (Soriano, 1999). Embryonic day 0.5 was defined as noon on the day of vagina plug. Six independent *Tbx1*-Cre founders exhibit identical staining patterns consistent with the known expression domain of *Tbx1*. Embryos were fixed in 2% PFA for 2 h and stained for β-galactosidase activity at 37°C. Images presented are representative of data obtained for all founders.

### *Generation of Tbx1-Cre::Fgf8$^{flox/-}$ embryos*

To generate *Tbx1*-domain tissue specific deletion of *Fgf8*, we utilized an allelic series of targeted mutations at the Fgf8 gene locus (Meyers et al., 1998). One parent in the mating is homozygous for an *Fgf8* allele in which exons 4 and 5 are flanked by loxP sites (*Fgf8*$^{flox/flox}$). The *Fgf8* null allele was generated by germline Cre-recombinase-mediated excision of exons 4 and 5 from the loxP allele. *Fgf8* heterozygotes were mated to *Tbx1*-Cre founders to generate *Tbx1*-Cre::*Fgf8*$^{+/-}$. Pups from appropriate intercrosses were harvested between 9.5 and 18.5 dpc or at birth and fixed 24–48 h in 4% paraformaldehyde.

### *Immunohistochemistry and histology*

Stained and unstained tissues or embryos were dehydrated through graded alcohol series, embedded in paraffin, and sectioned at 6–10 μM. Sections from embryos stained for β-galactosidase expression were counterstained with eosin. Neonatal heart-lung sections from *Tbx1*-Cre::*Fgf8*$^{flox/-}$ embryos were stained with hemotoxylin and eosin to α-actin expression (http://www.uphs.upenn.edu/mcrc). In situ hybridization was performed as described (Wawersik and Epstein, 2000).

### *Genotyping*

Genotyping was performed by PCR on DNA obtained from embryonic membranes or embryo tails. Primers, PCR conditions and genotyping protocols are available online at http://www.uphs.upenn.edu/mcrc.

## Results

### *Identification of conserved regions in the Tbx1 upstream genomic region between human and mouse*

Traditional enhancer analysis requires subcloning of large segments of genomic DNA and an iterative deletion scheme to identify individual enhancer regions. We chose instead to take advantage of the power of multispecies comparative sequence analysis to identify noncoding regions of homology. Using standard database techniques, we compared approximately 20 kb of DNA sequence upstream from the *Tbx1* start methionine between human and mouse by NCBI Blast2 (Altschul et al., 1997). We identified more than 10 regions of homology that ranged in size from approximately 50–250 bp (Fig. 1A). To assess the potential in vivo function of these elements, we cloned genomic fragments containing regions of conservation upstream of a *lacZ* reporter gene (Fig. 1B) and made F0 transient transgenic mice. These homologous regions were grouped to facilitate PCR based cloning of only four genomic fragments (Fig. 1A). Subsequent analysis of the same sequences with the VISTA sequence comparison program confirmed our original analysis and identified additional regions of somewhat lesser homology that were not included in our transgenic analysis (Fig. 1A) (Dubchak et al., 2000; Mayor et al., 2000). Comparative sequence analysis allowed us to eliminate nearly two thirds of the 20 kb of DNA examined before generating any transgenic animals (Dubchak et al., 2000; Mayor et al., 2000).

Within the proximal 3.1 kb of sequence upstream of the start ATG of *Tbx1*, significant regions are conserved between mouse and human; this region contains the minimal promoter and transcriptional start site(s) (Fig. 1B). However, this region was insufficient to direct expression of *lacZ* in eight transient transgenic embryos (Fig. 1, construct H). However, addition of three distinct regions that together contained most of the regions of significant homology within the proximal 16 kb of upstream sequence (Figs. 1A,B, construct A) was sufficient to recapitulate the endog-

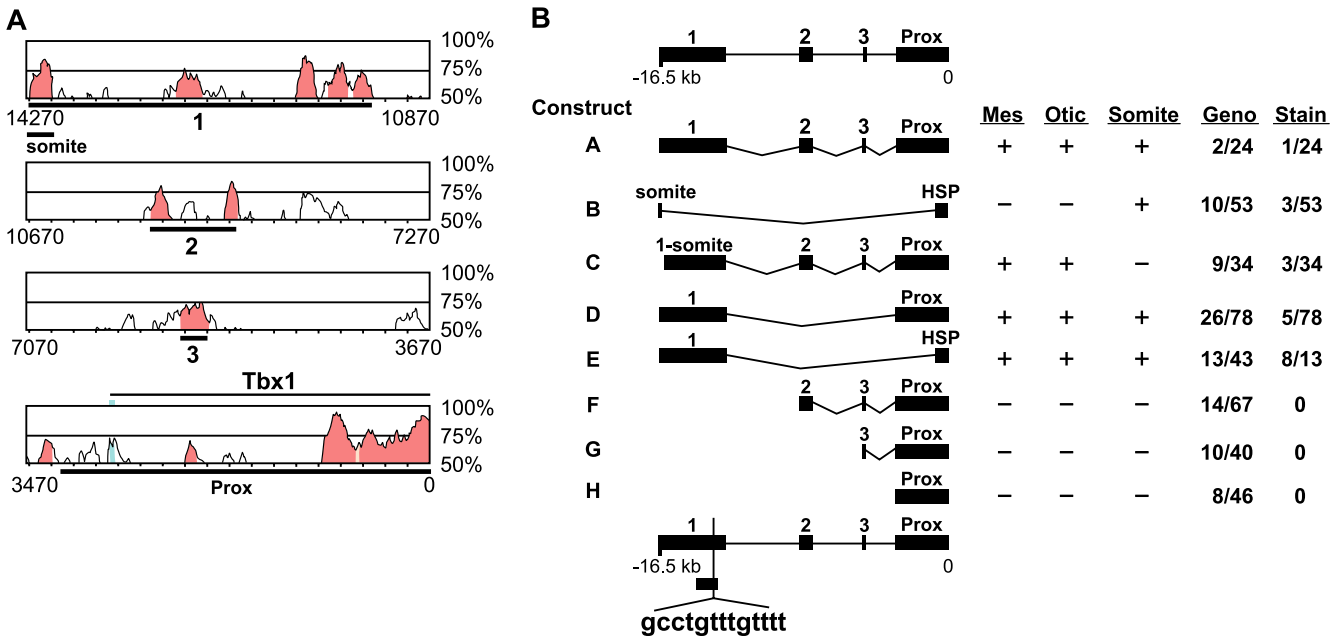


Fig. 1. *Tbx1* genomic comparisons and enhancer constructs. (A) VISTA alignment of mouse and human *Tbx1* genomic sequences. The *X*-axis is human sequence in base pairs from the start ATG. The *Y*-axis is percent identity with the corresponding mouse sequence. Pink elements represent regions of greater than 100 bp of >75% conserved sequence. The relative positions of subcloned fragments are indicated by black bars. (B) Stick diagrams indicate relative positions of fragments from mouse genomic sequence used for production of transgenic mice. Expression domains for each construct are indicated. Below, the position of a recently described 1.1-kb enhancer that drives expression in head mesenchyme and pharyngeal endoderm (Yamagishi et al., 2003) is indicated. The relative position of the conserved forkhead transcription factor binding site reported by Yamagishi et al. and its sequence are also shown.

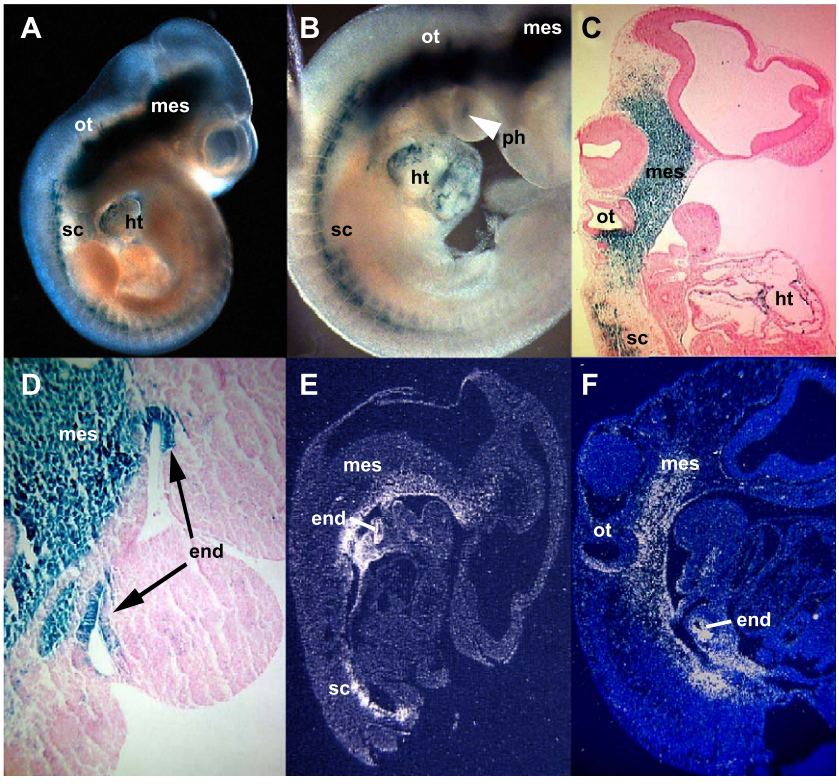


Fig. 2. Expression of *Tbx1-lacZ* construct A (depicted in Fig. 1B) and endogenous *Tbx1* at E10.5. (A, B) Expression is observed in mesenchyme (mes), otic vesicle (ot), sclerotome (sc), heart (ht), and pharyngeal mesenchyme (ph, white arrowhead). (C, D) Eosin-stained saggital sections through the same embryo in A. Note endoderm expression in (D), black arrows. (E, F) Analysis of *Tbx1* expression by radioactive in situ hybridization in E10.5 saggital sections. Note expression in mesenchyme (mes), otic vesicle (ot), endoderm (end), and sclerotome (sc) similar to expression in the transgenic embryo in C, D.

enous expression domain of *Tbx1* (Fig. 2). In two independently derived embryos, and in two subsequently developed stable transgenic lines, expression was evident in the head mesenchyme (Figs. 2A–D), the posterior region of the otic vesicle epithelium (Fig. 2C), the sclerotome (Figs. 2A–C), and pharyngeal endoderm (Fig. 2D). Expression was present in the core mesenchyme of the pharyngeal arches and in a subpopulation of myocardial cells in the heart (Figs. 2B,C). Each of these domains of expression represents endogenous regions of *Tbx1* expression as demonstrated by our laboratory (Figs. 2E,F) and others (Garg et al., 2001; Garvey et al., 1996). Hence, critical sequences required for most or all of *Tbx1* expression reside within regions of upstream homology (fragments 1–3, Fig. 1).

We constructed serial deletions of the 7.6-kb transgenic expression construct A by removing regions of sequence homology, as outlined in Fig. 1. Removal of the most upstream region (fragment 1, resulting in construct F, Fig. 1B) results in the complete loss of all expression at E10.5 (14 genotype positive embryos examined). Similarly, constructs containing only fragment 3 and the proximal element (construct G, Fig. 1B) failed to drive transgene expression in 10 transgenic embryos. A 207-bp element at the 5′ end of fragment 1 is sufficient to drive reporter expression in the somite (construct B, and Fig. 3A). Deletion of this somite element from construct A (producing construct C) eliminates somite expression but leaves other expression domains unaffected, thus demonstrating that this element is necessary

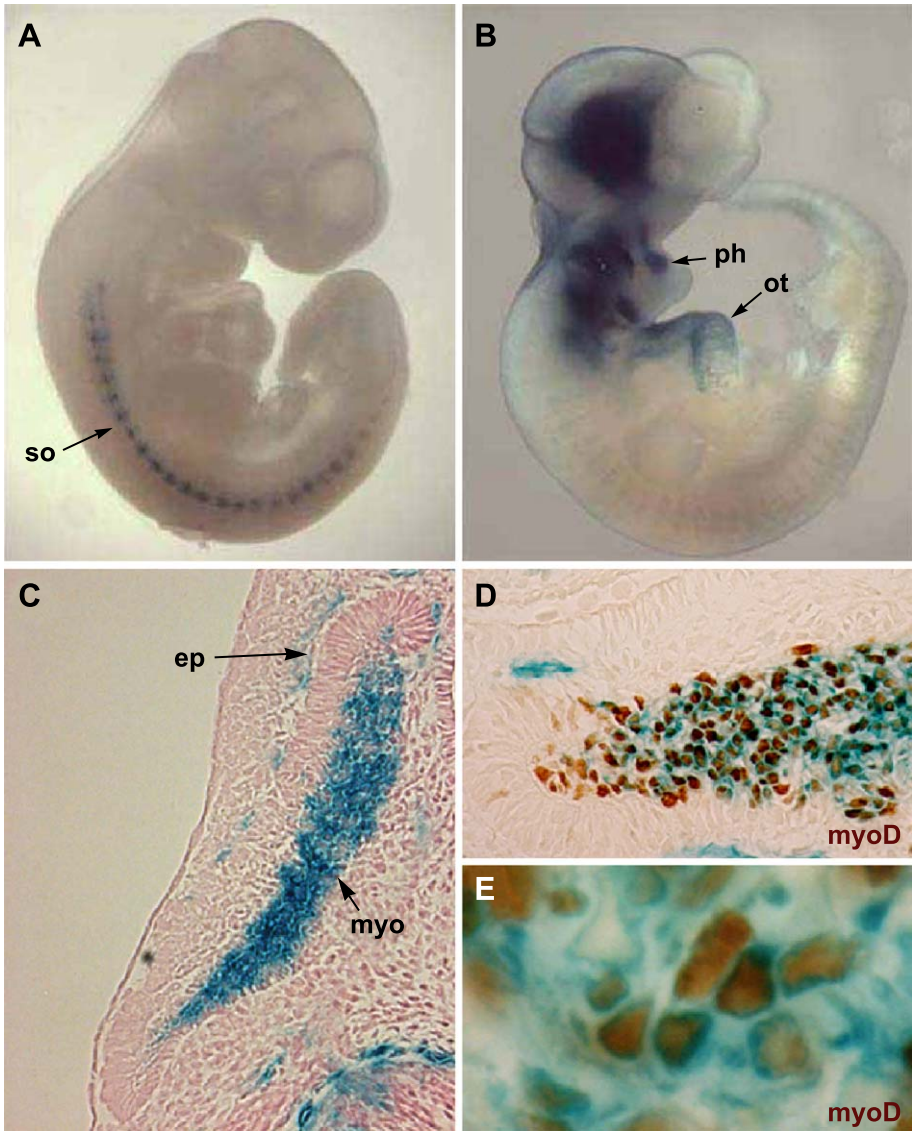


Fig. 3. Identification of a somite-specific enhancer element. (A) Somite (so)-specific expression obtained with construct B. (B) Loss of somite expression when the somite element is deleted from Fragment 1 yielding construct C. Expression is maintained in the pharyngeal core mesenchyme (ph) and cardiac outflow tract (ot). (C) Cross section of *Tbx1-lacZ* construct E embryo showing β-gal expression in the myotome (myo) but not in the epithelial portion of the somite (ep). β-gal expression colocalized with myoD (D). Higher power shows nuclear expression of myoD (brown) and cytoplasmic expression of β-galactosidase (blue) in the same cells (E).

and sufficient for somite expression (Fig. 3B). Somitic expression of *Tbx1-lacZ* was evident in the myotomal region of the somite, but not in the epithelial layer (Fig. 3C). Expression in myotomal cells was confirmed by costaining with a myoD antibody (Figs. 3D,E) and with an antibody to myosin (MF20, not shown).

Transgenic construct D, which utilizes only Fragment 1 attached to the *Tbx1* proximal element, recapitulates the entire *Tbx1* expression domain. This was also the case when Fragment 1 was attached to a heterologous HSP promoter (construct E). Thus, all of the sequences required for regulation of *Tbx1* expression are contained within the 3.5-kb Fragment 1. Previous reports have demonstrated that Tbx1 expression in pharyngeal mesenchyme and endoderm is genetically downstream of Sonic hedgehog (Shh) signaling (Garg et al., 2001). Consistent with these results, we observed down-regulation of Tbx1 transgene expression in Shh null embryos (Chiang et al., 1996) and ectopic Tbx1 expression in the periotic mesenchyme in a model of Shh overexpression (ShhP1) (Riccomagno et al., 2002) (data not shown). Shh may activate *Tbx1* indirectly by inducing expression of forkhead transcription factors (Yamagishi et al., 2003). A recent report demonstrated that sequences containing forkhead transcription factor binding sites, located at the 3′ end of our Fragment 1 (Fig. 1B), are responsible for expression in head mesenchyme and pharyngeal endoderm (but not pharyngeal mesoderm) (Yamagishi et al., 2003). Our results are consistent with this observation, although we have not yet directly confirmed the importance of the reported forkhead-binding site. Specific sequences required for expression in pharyngeal mesoderm and otic vesicle, while contained within Fragment 1, remain to be elucidated.

### *Characterization of transgenic mice expressing Cre recombinase in the Tbx1 expression domain and fate-mapping of Tbx1 descendents*

We used the *Tbx1* regulatory regions to create transgenic mice expressing Cre recombinase in *Tbx1* expression domains. We included all of the conserved regions depicted in Fig. 1B construct A. A total of six independent Cre-expressing transgenic lines were expanded and characterized. All six lines yielded consistent results, suggesting faithful expression of *Tbx1*-Cre in endogenous domains, unrelated to the site of transgene insertion. We refer to these as *Tbx1*-Cre mice.

We crossed *Tbx1*-Cre mice with R26R reporter mice that express *lacZ* constitutively in cells that express Cre recombinase (Soriano, 1999). Hence, the descendents of Cre-expressing cells can be identified by assaying for β-galactosidase activity even after Cre expression has itself subsided. We examined *Tbx1*-Cre::R26R embryos between E7.5 and birth (Fig. 4). Unexpectedly, at E7.5, we observed labeled cells in a pattern similar to the cardiac crescent where myocardial cells arise (Fig. 4A). By E8.5, labeled cells were identified in the pharyngeal region and head mesenchyme (Fig. 4B) though the heart tube was unlabeled. By E9.0–E9.5, β-galactosidase-expressing cells were seen in the outflow tract of the heart and the primordial of the right ventricle, but labeled cells were not seen in the left ventricle (Figs. 4C–E). *Tbx1* previously has been shown to be expressed by a few cardiac myocytes in the outflow tract of the heart (Vitelli et al., 2002a), and we observed a similar expression pattern in our *Tbx1-lacZ* embryos, but many cardiac myocytes in the heart at E9.5 do not express *Tbx1*. This indicates that cardiac myocytes in the outflow tract and right ventricle derive from *Tbx1*-expressing precursors that have subsequently extinguished *Tbx1* expression.

By E10.5, a few labeled cells were seen crossing the interventricular sulcus (arrow, Fig. 4G) and significant portions of the left ventricle were labeled by E14.5 (Fig. 4H) and in the adult heart (Fig. 4I) in addition to almost the entire right ventricle. Throughout development, labeled cells were also identified in pharyngeal endoderm and derivatives including the thymus (not shown). The pattern of expression during development of the heart, shown in Fig. 4, is consistent with expression of Tbx1 by progenitors of the recently described secondary (or anterior) heart field (Kelly and Buckingham, 2002; Kelly et al., 2001; Waldo et al., 2001).

We examined *Tbx1* gene expression by in situ hybridization at E7.5 (Fig. 5A) and E8.5 (Fig. 5C). At E7.5, *Tbx1* expression is evident in broad regions of the lateral plate mesoderm including cardiogenic regions (Fig. 5A). Expression partially overlaps with that of *Nkx2.5*, an early marker of cardiogenic cells (Fig. 5B). *Tbx1* appears to be expressed in a subset of cardiogenic precursors, consistent with our *Tbx1*-Cre fate-mapping experiments. By E8.5, endogenous*Tbx1* expression (Fig. 5C) is weak in the heart region, while *Nkx2.5* is abundantly expressed in the myocardium (Fig. 5D). To confirm that our *Tbx1*-Cre mice were expressing Cre recombinase is the same progenitors as those that express *Tbx1*, we performed in situ hybridization using adjacent sections from an E7.25 *Tbx1*-Cre embryo with *Tbx1* and *Cre* riboprobes (Figs. 5E,F). Expression of *Tbx1* and *Cre* were evident in the same population of early mesoderm, indicating that *Cre* expression accurately recapitulates endogenous expression of *Tbx1* in this tissue. Taken together, these results indicate that *Tbx1* is expressed very early and transiently in some cardiac progenitors that later give rise to the outflow tract myocardium, large portions of the right ventricle, and some portions of the left ventricle.

### *A subpopulation of vascular smooth muscle is derived from Tbx1-expressing cells*

In all of the *Tbx1*-Cre adult mice examined, we noted broad expression in the vasculature. Histological sections indicated that some vascular smooth muscle is derived from

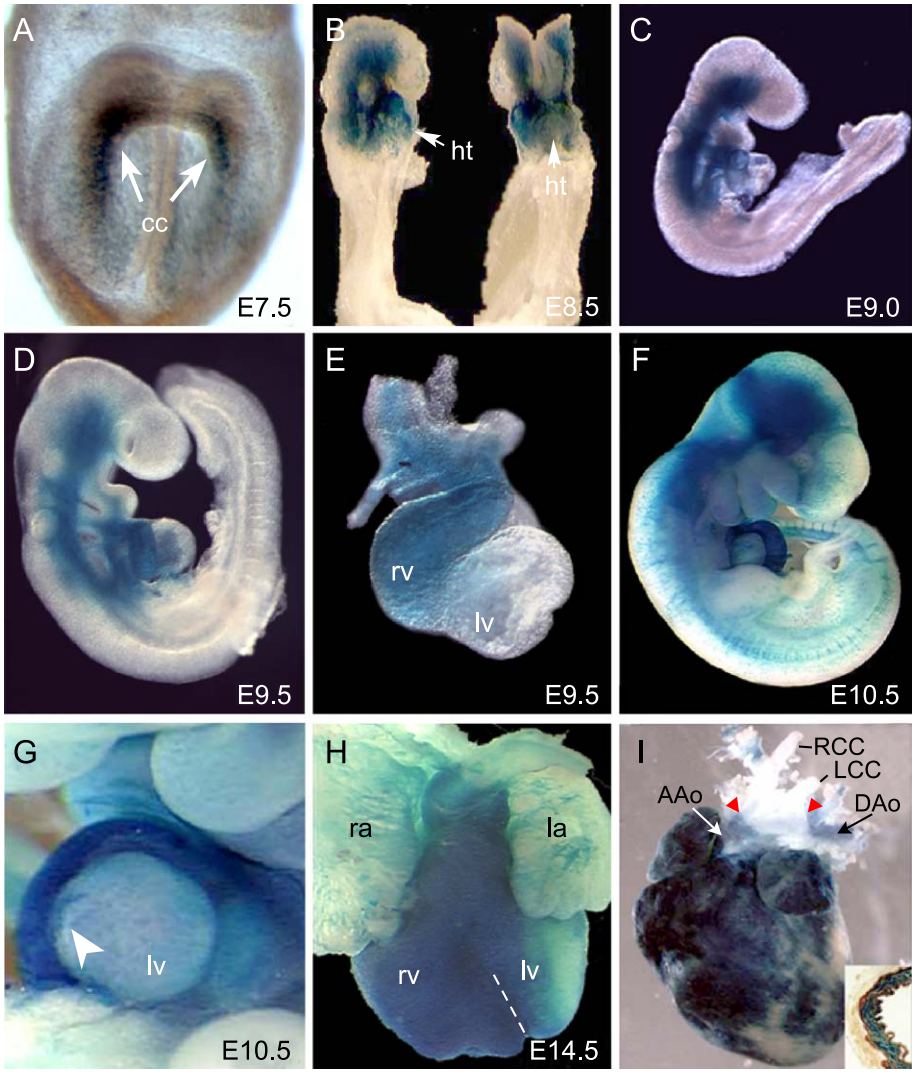


Fig. 4. Fate mapping of *Tbx1*-expressing cells. (A) At E7.5, expression of β-galactosidase is evident in the area of the cardiac crescent (cc) in *Tbx1*-Cre::R26R embryos. (B) At E8.5, expression is strong in the head mesenchyme but little expression is seen in the heart (ht). (C) At E9.0, expression is evident in the head mesenchyme, otic vesicle, and pharyngeal arch mesenchyme. Expression is also seen in the outflow tract of the heart. (D) By E9.5, expression has extended into the right ventricle. (E) Higher magnification of an E9.5 heart demonstrates restriction of blue cells to the right ventricle (rv) and conotruncus. (F) Right lateral view of an embryo at E10.5 showing strong expression in head mesenchyme and heart. Expression in the right atria is weak and spotty. (G) Left lateral high magnification view of the heart of the embryo in F. Strong expression is observed in the right ventricle and patches of expressing cells (white arrowhead) can be observed crossing the interventricular boundary into the left ventricle (lv). (H) At E14.5, the right ventricle appears to be almost completely derived from *Tbx1* descendants. Staining crosses the boundary between the right and left ventricles (dotted line) and significant regions of the left ventricle are stained. (I) Staining of the heart from an adult *Tbx1*-Cre::R26R mouse reveals extensive contribution from Cre-expressing progenitors throughout the myocardium with more extensive contribution to the right ventricle and atria compared with the left ventricle. β-galactosidase expression is detected in the ascending aorta (AAo) and descending aorta (DAo) but is absent from the aortic arch (between red arrowheads), the right common carotid (RCC), and left common carotid (LCC) arteries. A section through the descending aorta stained for smooth muscle α-actin (brown) demonstrates coexpression of this smooth muscle marker with β-galactosidase (I inset).

*Tbx1*-Cre expressing cells (Fig. 4I, inset). Interestingly, labeled smooth muscle was seen in the great vessels including the ascending aorta and the descending aorta beyond the ductus arteriosus. However, the aortic arch and the carotid arteries were not labeled (Fig. 4I). We have previously shown that smooth muscle in the aortic arch and carotid arteries derives from neural crest (Li et al., 2000). Hence, vascular smooth muscle is derived from lateral plate mesoderm, identified by *Tbx1*-Cre expression, and also from neural crest, identified by *Wnt1*-Cre (Jiang et al., 2000) and *Pax3*-Cre expression (Li et al., 2000). Taken together, these results suggest that *Tbx1* may play early roles in cardiac and smooth muscle development.

### *Targeted inactivation of Fgf8 in Tbx1 expression domains*

*Fgf8* signaling has recently been reported as a critical mediator of aortic arch development downstream of *Tbx1*

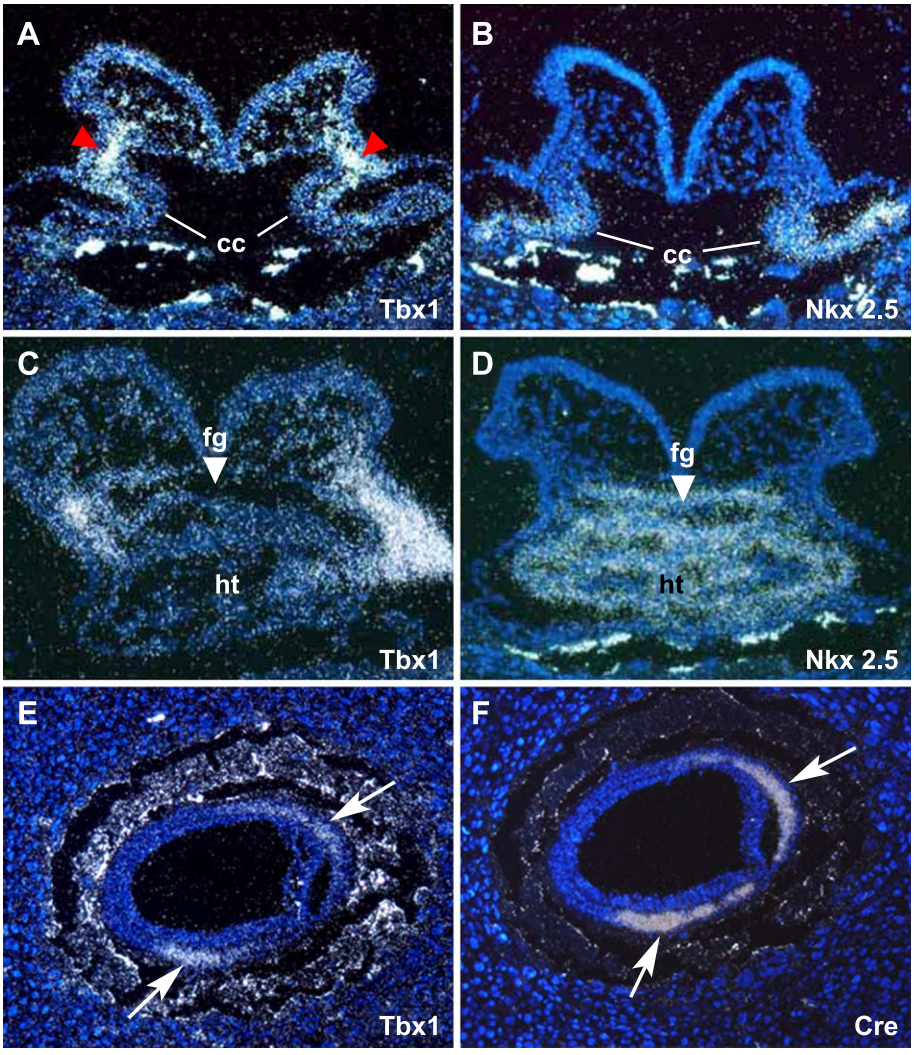


Fig. 5. Early cardiogenic expression of *Tbx1*. *Tbx1* expression was assessed by radioactive in situ hybridization at E7.5 (A) and E8.5 (C). *Tbx1* is expressed in the cardiac crescent (cc) at E7.5 (A), but expression is down-regulated in the heart tube (ht) at E8.5 (C). Early expression is also noted in the head mesenchyme (red arrows A). *Nkx2.5* is expressed in the cardiac crescent at E7.5 (B) and expression persists in the heart tube (ht) and foregut (fg) at E8.5 (D). Adjacent sections (E, F) of an E7.25 *Tbx1*-Cre embryo reveals expression of *Tbx1* (E) and *Cre* (F) in a subdomain of early mesoderm (arrows, E, F).

(Abu-Issa et al., 2002; Frank et al., 2002; Vitelli et al., 2002b). To perform tissue specific inactivation of *Fgf8* in the *Tbx1* expression domain, we took advantage of previously described *Fgf8* null ($Fgf8^{-/-}$) and loxP ($Fgf8^{flox}$) alleles (Meyers et al., 1998). In the loxP allele, *Fgf8* exons 4 and 5 are flanked by loxP sites. Cre-recombinase mediated excision generates a null allele in Cre-expressing tissues. Mice heterozygous for the *Fgf8* null allele were mated to *Tbx1*-Cre founders to generate compound heterozygotes (*Tbx1*-Cre::$Fgf8^{+/-}$). *Tbx1*-Cre::$Fgf8^{+/-}$ mice were mated to mice homozygous for an *Fgf8* loxP flanked allele ($Fgf8^{flox/flox}$). One quarter of the progeny from this mating are expected to be *Tbx1*-Cre::$Fgf8^{flox/-}$. Following Cre-mediated recombination at the loxP sites, these embryos are *Fgf8* null in the *Tbx1*-Cre expression domain.

To confirm specific loss of *Fgf8* signal in the *Tbx1* expression domain, we performed radioactive in situ hybridization on E10.5 wild type and *Tbx1*-Cre::$Fgf8^{flox/-}$ embryo sections. *Fgf8* signal is greatly reduced in pharyngeal endoderm of *Tbx1*-Cre::$Fgf8^{flox/-}$ embryos (Fig. 6B arrows, en) compared to a wild-type littermate (Fig. 6A). *Fgf8* expression is unaffected in the first arch ectoderm where *Tbx1* is not expressed (Figs. 6A,B white arrowhead, ec). These results confirm that *Tbx1*-Cre is functional within the normal *Tbx1* expression domain, and that loss of *Fgf8* signal is tissue-specific.

We examined litters derived from *Tbx1*-Cre::$Fgf8^{+/-}$ and $Fgf8^{flox/flox}$ crosses between E9.5 and birth. Between E9.5 and E15.5, we found the expected number of *Tbx1*-Cre::$Fgf8^{flox/-}$ embryos (27/115, 23.5%). By E18.5, we found an occasional nonviable *Tbx1*-Cre::$Fgf8^{flox/-}$ embryo, and at birth we identified numerous cyanotic *Tbx1*-Cre::$Fgf8^{flox/-}$ pups with irregular gasping breathing patterns that succumbed shortly after birth. At P1, we identified

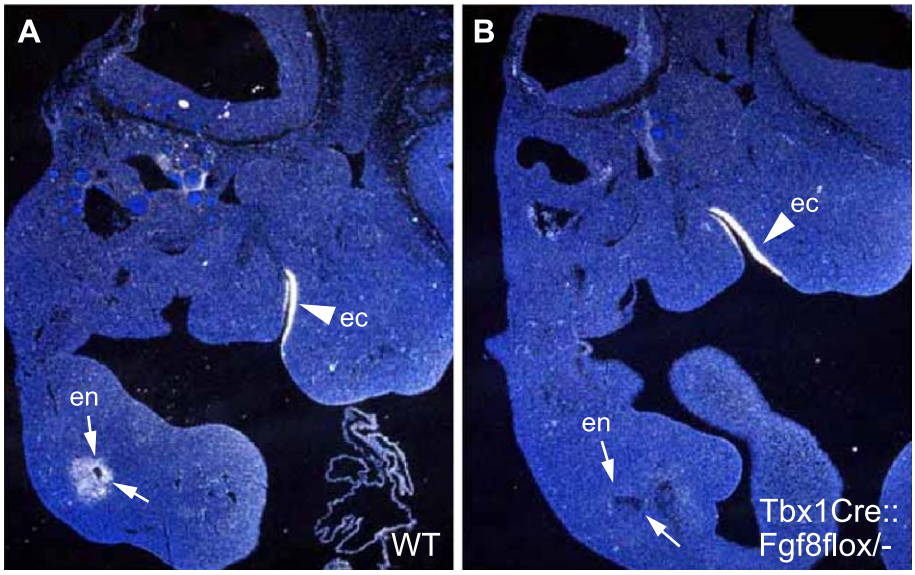


Fig. 6. *Fgf8* expression in *Tbx1*-Cre::*Fgf8*$^{flox/-}$ embryos. (A) *Fgf8* expression is observed in both endoderm (en) and ectoderm (ec) at E10.5 in wild-type embryos. (B) *Fgf8* expression is lost in the endodermal domain, but maintained in ectoderm in *Tbx1*-Cre::*Fgf8*$^{flox/-}$ embryos.

only 11 viable *Tbx1*-Cre::*Fgf8*$^{flox/-}$ pups of 118 genotypes (9% vs. 25% expected) indicating significant peri-natal lethality. Additionally, *Tbx1*-Cre::*Fgf8*$^{flox/-}$ pups were distinguishable following thoracotomy by reduced and/or single lobed thymus. Reduced thymus is also seen in Fgf8 hypomorphs and is consistent with removal of Fgf8 in the pharyngeal endoderm. However, the gross *Tbx1*-Cre::*Fgf8*$^{flox/-}$ phenotype was distinct from *Fgf8* hypomorphs, which display craniofacial defects (Abu-Issa et al., 2002; Frank et al., 2002), and from *Fgf8* nulls, which are early embryonic lethal (Meyers et al., 1998).

*Tbx1*-Cre::*Fgf8*$^{flox/-}$ embryos and newborn pups displayed cardiovascular patterning defects involving the outflow tract and proximal great vessels. These defects included malformations consistent with persistent truncus arteriosus, double outlet right ventricle, transposition of the great arteries, Tetrology of Fallot, atrial and ventricular septal defects and duplicated internal carotid arteries. Importantly, however, we never observed interruption of the aortic arch, right-sided aortic arch, or retro-esophageal right subclavian artery. This class of cardiovascular defect involves predominantly the aortic arch arteries without affecting the outflow tract of the heart, and are commonly seen in *Tbx1*$^{+/-}$ embryos, *Fgf8* hypomorphs, and in DiGeorge syndrome. Hence, inactivation of *Fgf8* in the *Tbx1* expression domain recapitulates some, but not all, of the cardiovascular defects related to *Tbx1* deficiency.

Normal great vessel morphology is displayed in Fig. 7A. The aorta (Ao) is dorsal to the pulmonary artery and the proximal arch elevates to the right. Cardiovascular defects observed in *Tbx1*-Cre::*Fgf8*$^{flox/-}$ animals include defects of conotruncal septation and malpositioning of the proximal great vessels. An example of malrotation of the great arteries is shown in Fig. 7B. In this animal, the aorta is positioned ventrally in a side-by-side presentation with the pulmonary artery (PA). The pulmonary artery overrides the left ventricle (Fig. 7F). Another *Tbx1*-Cre::*Fgf8*$^{flox/-}$ animal presented with transposition (Fig. 7C). In this individual, the aorta is ventral to the pulmonary artery (Fig. 7C). Hemotoxylin and eosin (H&E) staining of sections confirms an inappropriate ventral position of the aorta, and demonstrates that the aorta is in continuity with both ventricles through a large aortico-pulmonary window (AP, Fig. 7G). Several *Tbx1*-Cre::*Fgf8*$^{flox/-}$ pups presented with atrial septal defects (ASD, Fig. 7I) and membranous ventricular septal defects (VSD, Fig. 7J). One severely affected animal presented with a Tetrology of Fallot-like phenotype (Figs. 7D,H). This pup had a VSD and severe pulmonary atresia with no apparent pulmonary trunk arising from the right ventricle. The pulmonary arteries arose retrograde from the ductus arteriosus (DA-PA, Fig. 7D). This animal also exhibited a large arterial dissection filled with thrombus (Fig. 7H black arrows and Fig. 7L asterisk). The dissection can clearly be seen in Panel 7L underlying the endothelial layer that lines the aortic lumen.

Aortic dissection suggests a weakness of the arterial wall. H&E staining revealed morphological abnormalities of the arterial wall in *Tbx1*-Cre::*Fgf8*$^{flox/-}$ mice (black arrows, Fig. 7L) compared to wild type (Fig. 7K). The muscular wall was of variable thickness and lacked the striated structural appearance of normal arterial smooth muscle. This observation was confirmed by smooth muscle α-actin staining (SMA). Some smooth muscle staining is observed in the aortic wall of affected individuals (Fig. 7N). However, SMA expression is not observed in the stereotypic striated layers expected for mature arterial smooth muscle as seen in wild-type aorta (Fig. 7M). Defective smooth muscle differentiation was a consistent finding in most *Tbx1*-

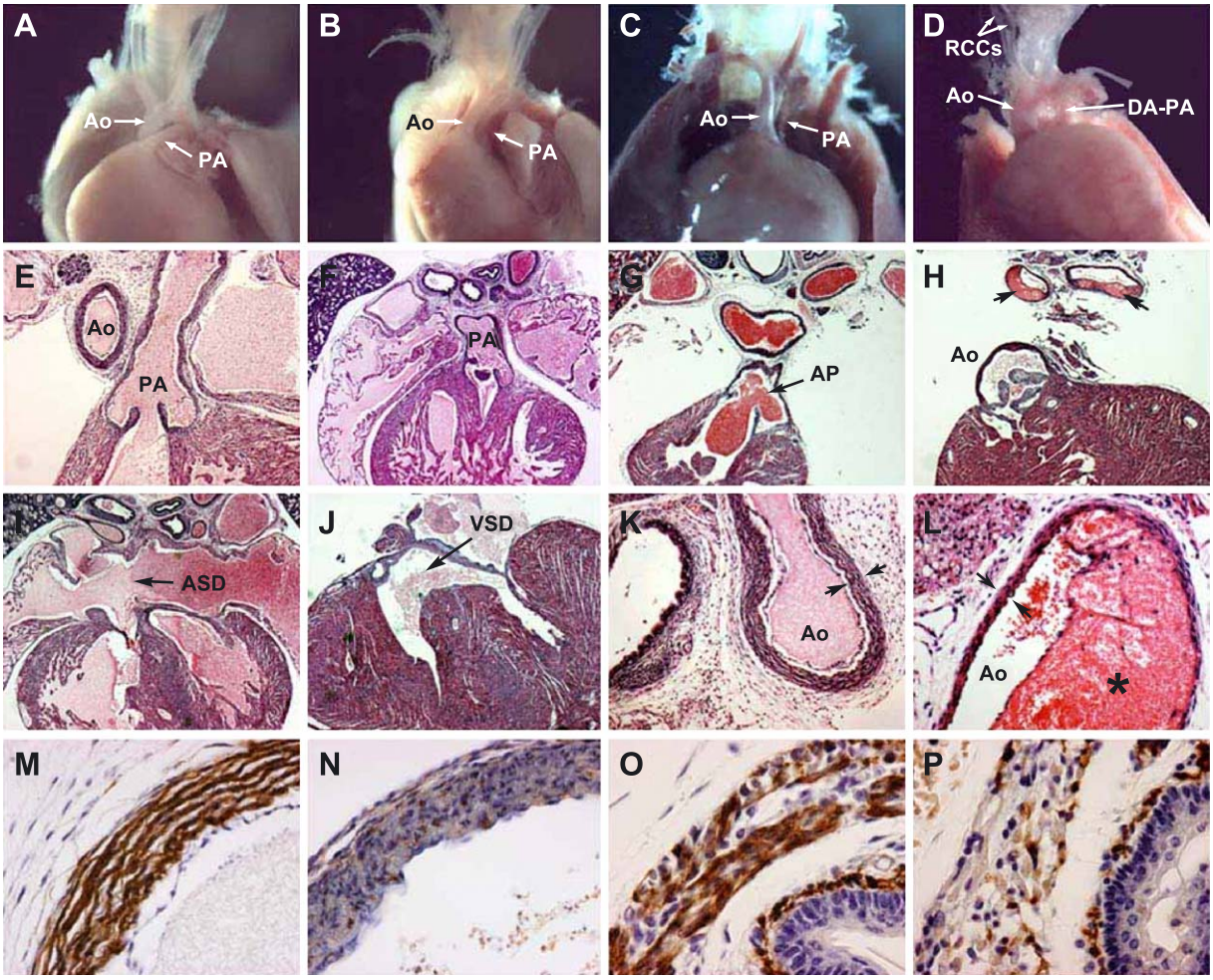


Fig. 7. Congenital heart disease in *Tbx1*-Cre::*Fgf8*$^{flox/-}$ mice. (A) Wild-type newborn heart after removal of the atria to reveal the outflow tract, aorta (Ao), and pulmonary artery (PA). (B–D) Mutant embryos with malrotation (B), transposition of the great arteries (TGA) (C), and absent proximal pulmonary artery (D). In D, the pulmonary artery fills retrograde from the ductus arteriosus (DA–PA). The right common carotid artery is duplicated (RCCs). (E) H&E transverse section of a wild-type heart at the level of the pulmonary valve. (F) Transverse section of the heart shown in B showing overriding pulmonary artery. (G) Section of the heart shown in C revealing a large aortico-pulmonary window (AP) and the pulmonary artery dorsal to the aorta consistent with TGA. (H) Section of the heart in D showing absence of the proximal pulmonary artery. (Arrows indicate a large clot-filled dissection of the arterial wall). (I) A representative section from a *Tbx1*-Cre::*Fgf8*$^{flox/-}$ animal exhibiting a large atrial septal defect (ASD). (J) An example of ventricular septal defect in *Tbx1*-Cre::*Fgf8*$^{flox/-}$. (K) H&E section of the aortic arch in wild-type newborn. (L) Aortic arch of the heart shown in D. Note the large dissection (*) lined by endothelium, and the thin arterial wall (arrows). (M) Smooth muscle α-actin (SMA, brown) stained wild-type aorta. (N) SMA-stained aorta from heart shown in D. Note low levels of SMA expression and lack of normal smooth muscle architecture. (O) SMA-stained esophagus of wild-type newborn. (P) SMA-stained esophagus of affected newborn.

Cre::*Fgf8*$^{flox/-}$ animals. Unexpectedly, defective smooth muscle differentiation is also observed in the esophagus (Figs. 7O,P). SMA expression is greatly reduced (Fig. 7P) compared to wild type (Fig. 7O), though mesenchymal appearing cells are present.

## Discussion

### *Tbx1 and Fgf8 in cardiovascular development*

A growing body of data has implicated roles for both *Tbx1* and *Fgf8* during cardiac outflow tract development and aortic arch remodeling. Mutations in either gene can result in similar cardiovascular phenotypes, and compound heterozygotes have more severe defects than either heterozygote alone (Vitelli et al., 2002b). Both *Fgf8* and *Fgf10* expression levels are decreased in *Tbx1*-deficient embryos, suggesting that Fgf signaling functions downstream of *Tbx1* (Frank et al., 2002; Vitelli et al., 2002b). Here, we provide direct evidence that inactivation of *Fgf8* in *Tbx1*-expressing cells results in DiGeorge-like cardiovascular defects. These abnormalities are associated with a striking defect in smooth muscle differentiation. Arterial smooth muscle is derived from different embryonic origins. Smooth muscle of the aortic arch and ductus arteriosus is derived from neural crest cells (Jiang et al., 2000; Li et al., 2000). Smooth muscle of the proximal aorta, pulmonary trunk, and descending aorta

are mesodermally derived. Interestingly, defects present in our *Tbx1*-Cre::*Fgf8*$^{flox/-}$ embryos are not restricted to the neural crest-derived portions of the aortic arch. This indicates that smooth muscle differentiation in the aortic arches is dependent on the source and proximity of Fgf8 expression. Our results argue that endodermal Fgf8 expression is required for smooth muscle differentiation in proximal aorta and pulmonary trunk. Due to the absence of aortic arch interruptions, which are present in Fgf8 hypomorphs (Abu-Issa et al., 2002), we propose that Fgf8 produced from a non-Tbx1-regulated site, such as the ectoderm, may play a larger role in the differentiation and maintenance of smooth muscle populations within the arch proper. Additionally, we observed an unexpected decrease in smooth muscle differentiation in the esophagus. These observations suggest that *Fgf8* signaling plays a crucial role in the differentiation of a broad range of pharyngeal smooth muscle. Further analysis will provide insight into the role of *Fgf8* signaling in the maintenance and differentiation of smooth muscle in diverse tissues and of diverse embryonic origins.

Haploinsufficiency of *Tbx1* results in cardiovascular defects that include septation outflow tract defects as well as interruptions of the aortic arch and other abnormalities related to inappropriate regression of aortic arch segments. Similar malformations are seen in Fgf8 hypomorphic mutant mice. Strikingly, however, we did not observe interruptions of the aortic arch in our *Tbx1*-Cre::*Fgf8*$^{flox/-}$ mice. Thus, interruptions of the aortic arch in Fgf8 hypomorphic mice may be due to deficient Fgf8 signaling that derives from tissues that do not express *Tbx1*. Consistent with this idea, recent results suggest that inactivation of Fgf8 in pharyngeal ectoderm results in aortic arch interruptions but not outflow tract defects (Macatee et al., 2003). Aortic arch defects present in *Tbx1*$^{+/-}$ mice may be caused by an unrelated mechanism, perhaps involving Fgf10 or other signaling pathways.

### *Tbx1 and the secondary heart field*

Fate-mapping studies described here using *Tbx1*-Cre mice indicate that this transgene is expressed by early mesodermal derivatives in the lateral and intermediate plate, including precursors of cardiac and smooth muscle. Somitic derivatives, including skeletal muscle, also derive from Cre-expressing precursors in these studies (not shown). In situ expression analysis of endogenous *Tbx1* is consistent with early expression in these tissues followed by rapid restriction to more precise cell populations early during gestation. Early expression in a broad range of mesodermal progenitors has not been previously suggested, though persistent expression in a small population of cardiac myocytes in the outflow tract has been reported (Vitelli et al., 2002a). Other members of the T-box family are expressed in early mesoderm, suggesting the likelihood of functional redundancy (Garvey et al., 1996). For instance, T (brachyury) is one of the earliest markers of mesoderm and is expressed by all early mesodermal cell types (Wilson et al., 1995). Tbx5 is expressed by cardiogenic precursors and mutations in *TBX5* cause Holt–Oram syndrome, which includes cardiac malformations (Li et al., 1997). It is interesting to note that while *Tbx1* and *Tbx5* expression domains appear to overlap in early cardiogenic mesoderm, the expression domains in the heart at later time points are reciprocal (Bruneau et al., 1999). Tbx5 is expressed in the left ventricle and atria from the looped heart tube stage onward while our results indicate Tbx1 progeny are predominantly restricted to the right ventricle (Bruneau et al., 1999). It will be interesting to determine if Tbx1 serves overlapping and/or redundant functions with other T-box family members during early mesoderm differentiation, and how these functions may change in the specification of cardiac cell fates later in development.

We were surprised by the pattern and extent of cardiac myocyte derivation from *Tbx1*-expressing precursors. At the cardiac crescent stage, we identified *Tbx1*-Cre derived cells in the region of cardiomyogenic precursors, and *Tbx1* expression itself partially overlapped with that of *Nkx2.5*. Shortly thereafter, *Tbx1*-Cre-derived cells populated the pharyngeal region, the outflow tract of the heart, and subsequently the right ventricle. This pattern of expression is highly reminiscent of the recently described secondary or anterior heart field (Kelly and Buckingham, 2002; Kelly et al., 2001; Waldo et al., 2001). All or most cardiac myocytes had been thought to arise from the primary heart field, which is identified by early expression of *Nkx2.5* and other early cardiac markers. However, recent data suggests that portions of the outflow tract and right ventricle may arise from a secondary field located more anteriorly. The extent of contribution of this secondary heart field to the mature heart remains controversial, and may vary between species. Our data suggests that the secondary heart field may be identified by expression of *Tbx1* and may originate near the cardiac crescent. The extent of contribution to the mature heart could depend on the precise markers used to differentiate the two heart fields within a region that initially represents a continuum of adjacent tissue. Hence, at the cardiac crescent stage, *Nkx2.5* may label both heart fields, while *Tbx1* is predominantly restricted to a subpopulation of precursors destined to be the secondary heart field.

Our results would argue for a significant contribution of *Tbx1*-expressing precursors to both the right and left ventricles. Intriguingly, the contribution of *Tbx1* progeny to the myocardium appears to increase as the heart develops. This increase in myocardial chimerism as cardiac development proceeds may reflect displacement of cells from the primary heart field by cells of the secondary heart field. This would imply a much more invasive role for cells of the secondary heart field than has been previously noted. Labeled cells appear in the left ventricular myocardium after it is formed and are not simply added to the heart sequentially from a population of pharyngeal mesoderm. Alternatively, the early

heart may be chimeric at an undetectable level, and apparent increases in chimerism over time is therefore due to clonal expansion of individual cells of different embryonic origin. Given the early mesodermal expression of *Tbx1* and its later expression in pharyngeal tissues, it will be of interest to determine which cardiac precursor populations express *Tbx1* and if it plays a functional role in cardiac muscle maturation. In this regard, it is noteworthy that some mouse models of DiGeorge syndrome have a thinned and poorly developed myocardium (Merscher et al., 2001). Hence, some aspects of the *Tbx1*-deficient phenotype and DiGeorge syndrome could be related to a cell-autonomous role of *Tbx1* in cardiac and other mesodermal progenitors.

### *Tbx1 and DiGeorge syndrome*

Although *TBX1* is an attractive candidate gene for cardiovascular defects in DiGeorge syndrome, no missense mutations have been discovered in patients with congenital heart disease or DiGeorge syndrome who do not have deletions on 22q11 (Han et al., 2001). If *TBX1* deficiency alone is responsible for cardiovascular malformations in this syndrome, it is surprising that mutations in the coding region have not been identified. It is possible that deletion of small regions on chromosome 22 results in inactivation of *TBX1* in addition to another gene that contributes to the phenotype or compensates for otherwise lethal effects of *TBX1* mutation (Guris et al., 2001; Yamagishi et al., 1999). If so, hypomorphic mutations in *TBX1* will possibly be associated with congenital cardiac disorders. Additionally, both over- and under- expression of *Tbx1* in mice results in cardiovascular malformations (Merscher et al., 2001). Mutations within specific regulatory regions might reduce, or expand, *TBX1* gene expression in critical tissues resulting in developmental defects in the absence of coding mutations. Therefore, it is noteworthy that the enhancer regions that we have identified are generally conserved between mouse and human. It will be of interest to determine if mutations in these regulatory regions are found in human cases of non-deleted DiGeorge syndrome or in other cases of congenital heart disease.

The observation that inactivation of *Fgf8* in the *Tbx1* expression domain recapitulates some, but not all, of the cardiovascular manifestations of DiGeorge syndrome is consistent with a role for Fgf8 downstream of Tbx1. This interpretation is supported by prior data that indicates down-regulation of *Fgf8* in embryos lacking *Tbx1*, but additional studies will be required to determine if *Fgf8* is a direct downstream transcriptional target of Tbx1. However, our data suggests that additional targets of Tbx1 must also function during cardiovascular development since some characteristic malformations, including interruptions of the aortic arch, were not seen in our studies. Likewise, the presence of a complete array of DiGeorge-like cardiovascular malformations in Fgf8 hypomorphs, which are not recapitulated entirely by tissue-specific inactivation of *Fgf8* in Tbx1-expressing cells, indicates that there are mechanisms unrelated to Tbx1 function that can result in the DiGeorge cardiovascular phenotype.

## Acknowledgments

We thank members of the Epstein lab for helpful suggestions. This work was supported by NIH RO1 HL61475, F32 AR08584 and the American Heart Association, and R01 HD420803 to ENM.

## References

Abu-Issa, R., Smyth, G., Smoak, I., Yamamura, K., Meyers, E.N., 2002. Fgf8 is required for pharyngeal arch and cardiovascular development in the mouse. Development 129, 4613–4625.

Altschul, S.F., Madden, T.L., Schaffer, A.A., Zhang, J., Zhang, Z., Miller, W., Lipman, D.J., 1997. Gapped BLAST and PSI-BLAST: a new generation of protein database search programs. Nucleic Acids Res. 25, 3389–3402.

Bruneau, B.G., Logan, M., Davis, N., Levi, T., Tabin, C.J., Seidman, J.G., Seidman, C.E., 1999. Chamber-specific cardiac expression of *Tbx5* and heart defects in Holt–Oram syndrome. Dev. Biol. 211, 100–108.

Chiang, C., Litingtung, Y., Lee, E., Young, K.E., Corden, J.L., Westphal, H., Beachy, P.A., 1996. Cyclopia and defective axial patterning in mice lacking Sonic hedgehog gene function. Nature 383, 407–413.

Dubchak, I., Brudno, M., Loots, G.G., Pachter, L., Mayor, C., Rubin, E.M., Frazer, K.A., 2000. Active conservation of noncoding sequences revealed by three-way species comparisons. Genome Res. 10, 1304–1306.

Epstein, J.A., 2001. Developing models of DiGeorge syndrome. Trends Genet. 17, S13–S17.

Frank, D.U., Fotheringham, L.K., Brewer, J.A., Muglia, L.J., Tristani-Firouzi, M., Capecchi, M.R., Moon, A.M., 2002. An Fgf8 mouse mutant phenocopies human 22q11 deletion syndrome. Development 129, 4591–4603.

Garg, V., Yamagishi, C., Hu, T., Kathiriya, I.S., Yamagishi, H., Srivastava, D., 2001. Tbx1, a DiGeorge syndrome candidate gene, is regulated by sonic hedgehog during pharyngeal arch development. Dev. Biol. 235, 62–73.

Garvey, N., Hancock, S., Ruvinsky, I., Chapman, D.L., Agulnik, I., Bollag, R., Papaioannou, V., Silver, L.M., 1996. Expression of the T-box family genes, Tbx1–Tbx5, during early mouse development. Genetics 144, 249–254.

Goldmuntz, E., Emanuel, B.S., 1997. Genetic disorders of cardiac morphogenesis. The DiGeorge and velocardiofacial syndromes. Circ. Res. 80, 437–443.

Graham, A., 2001. The development and evolution of the pharyngeal arches. J. Anat. 199, 133–141.

Graham, A., Smith, A., 2001. Patterning the pharyngeal arches. BioEssays 23, 54–61.

Guris, D.L., Fantes, J., Tara, D., Druker, B.J., Imamoto, A., 2001. Mice lacking the homologue of the human 22q11.2 gene CRKL phenocopy neurocristopathies of DiGeorge syndrome. Nat. Genet. 27, 293–298.

Han, E.J., Heng, C.K., Gong, W.K., Gong, W., 2001. Mutation analysis of TBX1 in non-deleted patients with features of DGS/VCFS or isolated cardiovascular defects. Pediatr. Nephrol. 16, 1049–1052.

Hiruma, T., Nakajima, Y., Nakamura, H., 2002. Development of pharyngeal arch arteries in early mouse embryo. J. Anat. 201, 15–29.

Jerome, L.A., Papaioannou, V.E., 2001. DiGeorge syndrome phenotype in mice mutant for the T-box gene, Tbx1. J. Child Adolesc. Psychopharmacol. 11, 109.

Jiang, X., Rowitch, D.H., Soriano, P., McMahon, A.P., Sucov, H.M., 2000. Fate of the mammalian cardiac neural crest. Development 127, 1607–1616.

Johnson, R.L., Riddle, R.D., Tabin, C.J., 1994. Mechanisms of limb patterning. Curr. Opin. Genet. Dev. 4, 535–542.

Kelly, R.G., Buckingham, M.E., 2002. The anterior heart-forming field: voyage to the arterial pole of the heart. Trends Genet. 18, 210–216.

Kelly, R.G., Brown, N.A., Buckingham, M.E., 2001. The arterial pole of the mouse heart forms from Fgf10-expressing cells in pharyngeal mesoderm. Dev. Cell 1, 435–440.

Kochilas, L., Merscher-Gomez, S., Lu, M.M., Potluri, V., Liao, J., Kucherlapati, R., Morrow, B., Epstein, J.A., 2002. The role of neural crest during cardiac development in a mouse model of DiGeorge syndrome. Dev. Biol. 251, 157–166.

Li, Q.Y., Newbury-Ecob, R.A., Terrett, J.A., Wilson, D.I., Curtis, A.R., Yi, C.H., Gebuhr, T., Bullen, P.J., Robson, S.C., Strachan, T., et al., 1997. Holt–Oram syndrome is caused by mutations in TBX5, a member of the Brachyury (T) gene family. Nat. Genet. 15, 21–29.

Li, J., Chen, F., Epstein, J.A., 2000. Neural crest expression of Cre recombinase directed by the proximal Pax3 promoter in transgenic mice. Genesis 26, 162–164.

Lindsay, E.A., Vitelli, F., Su, H., Morishima, M., Huynh, T., Pramparo, T., Jurecic, V., Ogunrinu, G., Sutherland, H.F., Scambler, P.J., et al., 2001. Tbx1 haploinsufficiency in the DiGeorge syndrome region causes aortic arch defects in mice. Nature 410, 97–101.

Macatee, T.L., Hammond, B.P., Arenkiel, B.R., Francis, L., Frank, D.U., Moon, A.M., 2003. Ablation of specific expression domains reveals discrete functions of ectoderm- and endoderm- derived FGF8 during cardiovascular and pharyngeal development. Development 130, 6361–6374.

Mayor, C., Brudno, M., Schwartz, J.R., Poliakov, A., Rubin, E.M., Frazer, K.A., Pachter, L.S., Dubchak, I., 2000. VISTA: visualizing global DNA sequence alignments of arbitrary length. Bioinformatics 16, 1046–1047.

Merscher, S., Funke, B., Epstein, J.A., Heyer, J., Puech, A., Lu, M.M., Xavier, R.J., Demay, M.B., Russell, R.G., Factor, S., et al., 2001. TBX1 is responsible for cardiovascular defects in velo-cardio-facial/DiGeorge syndrome. Cell 104, 619–629.

Meyers, E.N., Lewandoski, M., Martin, G.R., 1998. An Fgf8 mutant allelic series generated by Cre- and Flp-mediated recombination. Nat. Genet. 18, 136–141.

Riccomagno, M.M., Martinu, L., Mulheisen, M., Wu, D.K., Epstein, D.J., 2002. Specification of the mammalian cochlea is dependent on Sonic hedgehog. Genes Dev. 16, 2365–2378.

Soriano, P., 1999. Generalized lacZ expression with the ROSA26 Cre reporter strain. Nat. Genet. 21, 70–71.

Vitelli, F., Morishima, M., Taddei, I., Lindsay, E.A., Baldini, A., 2002a. Tbx1 mutation causes multiple cardiovascular defects and disrupts neural crest and cranial nerve migratory pathways. Hum. Mol. Genet. 11, 915–922.

Vitelli, F., Taddei, I., Morishima, M., Meyers, E.N., Lindsay, E.A., Baldini, A., 2002b. A genetic link between Tbx1 and fibroblast growth factor signaling. Development 129, 4605–4611.

Waldo, K.L., Kumiski, D.H., Wallis, K.T., Stadt, H.A., Hutson, M.R., Platt, D.H., Kirby, M.L., 2001. Conotruncal myocardium arises from a secondary heart field. Development 128, 3179–3188.

Wawersik, S., Epstein, J.A., 2000. Gene expression analysis by in situ hybridization. Radioactive probes. Methods Mol. Biol. 137, 87–96.

Wilson, V., Manson, L., Skarnes, W.C., Beddington, R.S., 1995. The T gene is necessary for normal mesodermal morphogenetic cell movements during gastrulation. Development 121, 877–886.

Yamagishi, H., Garg, V., Matsuoka, R., Thomas, T., Srivastava, D., 1999. A molecular pathway revealing a genetic basis for human cardiac and craniofacial defects. Science 283, 1158–1161.

Yamagishi, H., Maeda, J., Hu, T., McAnally, J., Conway, S.J., Kume, T., Meyers, E.N., Yamagishi, C., Srivastava, D., 2003. Tbx1 is regulated by tissue-specific forkhead proteins through a common Sonic hedgehog-responsive enhancer. Genes Dev. 17, 269–281.